SLAC National Accelerator Lab
LCLS-II TN-15-09
April 2015

Feeding the SXR Undulator with the CuRF Electron Beam: Option for LCLS-II

G. Marcus*, H. D. Nuhn, T. Raubenheimer

SLAC, Menlo Park, CA 94025

Abstract

The production of high peak power and high peak flux FEL pulses in the soft X-ray spectral range at LCLS-II is an attractive option. This technical note details a study of the production of such pulses by feeding the soft X-ray undulator with the high power, low repetition rate electron beam from the existing LCLS copper linac.

*gmarcus@slac.stanford.edu

1 Introduction

The LCLS-II undulator beamlines, one to support the production of hard X-rays (HXR) and one to support the production of soft X-rays (SXR), will nominally be fed by a high repetition rate electron beam coming from a continuous wave, superconducting radio frequency (CW SCRF) linac to cover the photon tuning range from 200 eV to 5 keV in the baseline configuration. These beamlines will also incorporate self-seeded infrastructure to provide bandwidth and pulse length tuning flexibility. Additionally, the existing LCLS copper (CuRF) linac will deliver beam to the HXR undulator to support lasing up to at least 25 keV. Potential users from a recent LCLS-II scientific opportunities workshop have inquired about the possibility of feeding the SXR undulator with the electron beam produced by the CuRF linac. The marriage of a high power electron beam with a large K undulator is suitable for producing high peak power and high peak flux FEL pulses.

We explore the possibility of feeding the SXR undulator with the high power electron beam produced by the CuRF linac. Tuning curves based on semi-analytic estimates, which includes empirically derived undulator taper scalings, are presented. Furthermore, quasi-start-to-end simulations detailing the production of high power FEL pulses at the high end of the tuning range, $E_\gamma = 1.5$ keV, are presented and show impressive overall performance.

2 SXR FEL Performance

The combination of a high power electron beam with a large K (undulator parameter) undulator allows for the production of high power FEL pulses. The potential of these high peak power pulses, from the user perspective, offers a compelling reason to feed the SXR undulator with the low repetition rate electron beam from the CuRF linac. The performance of this scheme is discussed below.

2.1 Beamline geometry

The baseline LCLS-II SXR undulator nominally consists of 21 individual undulator segments, the parameters of which can be found in Table 1. The SXR undulator beamline will

Table 1: Nominal SXR undulator parameters.

Paramter	**Symbol**	**Value**	**Unit**
undulator type	-	Hybrid PM, planar	x-pol
undulator period	λ_u	39	mm
segment length	L_u	3.4	m
break length	L_b	1.0	m
# segments	N_u	21	-
total length	L_{tot}	96	m

also support self-seeding across the entire tuning range with the high rep-rate SCRF linac produced electron beam. As such, there is a break at the location where the 8th undulator segment would nominally exist in order to host the grating based monochromator and electron beam bypass chicane. This section is not modeled here in the start-to-end simulations as it has no relevant impact.

2.2 Electron beam properties

Semi-analytic estimates, as well as quasi-start-to-end (S2E) numerical particle simulations, are used to evaluate the performance of the SXR FEL with the high power electron beam. Particles are tracked using `ASTRA` and `ELEGANT` from the LCLS injector to the entrance of the bypass that would take the LCLS electron beam to the LCLS-II SXR undulator (hence the term quasi). Future studies will evaluate the impact of the additional electron beam transport on the FEL performance. Figure 1 shows the detailed slice properties of a 180 pC electron beam used for this study. The current in the core of the beam is roughly $I \sim 2.5$

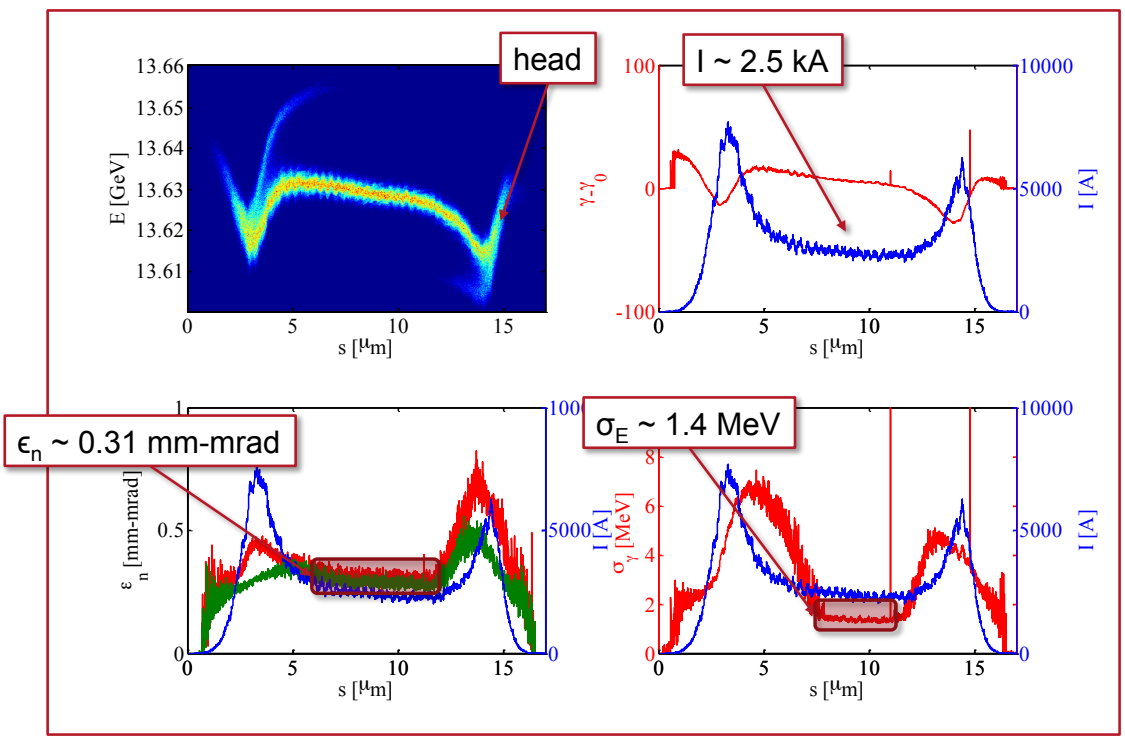

Figure 1: Top left: Longitudinal phase space. Top right: Current (blue) and slice energy (red). Bottom left: Current (blue), slice emittance (green - x, red - y). Bottom right: Current (blue), rms slice energy spread (red).

kA while the normalized slice emittance is $\epsilon_{n,(x,y)} \sim 0.31$ mm-mrad and the rms slice energy spread is $\sigma_E \sim 1.4$ MeV. This electron beam is an accurate representation of the nominal operating conditions at LCLS. While the longitudinal phase space (top left of Figure 1)

shows an energy of $\sim$ 13.6 GeV, the energy used in the simulations is $\sim$ 10 GeV. `GENESIS` is used to simulate the FEL performance with this S2E particle distribution.

2.3 Semi-analytic estimates

The estimated SXR FEL performance, including a post-saturation taper, is shown in Figure 2. Here, the FEL pulse intensity is shown as a function of both the electron beam energy

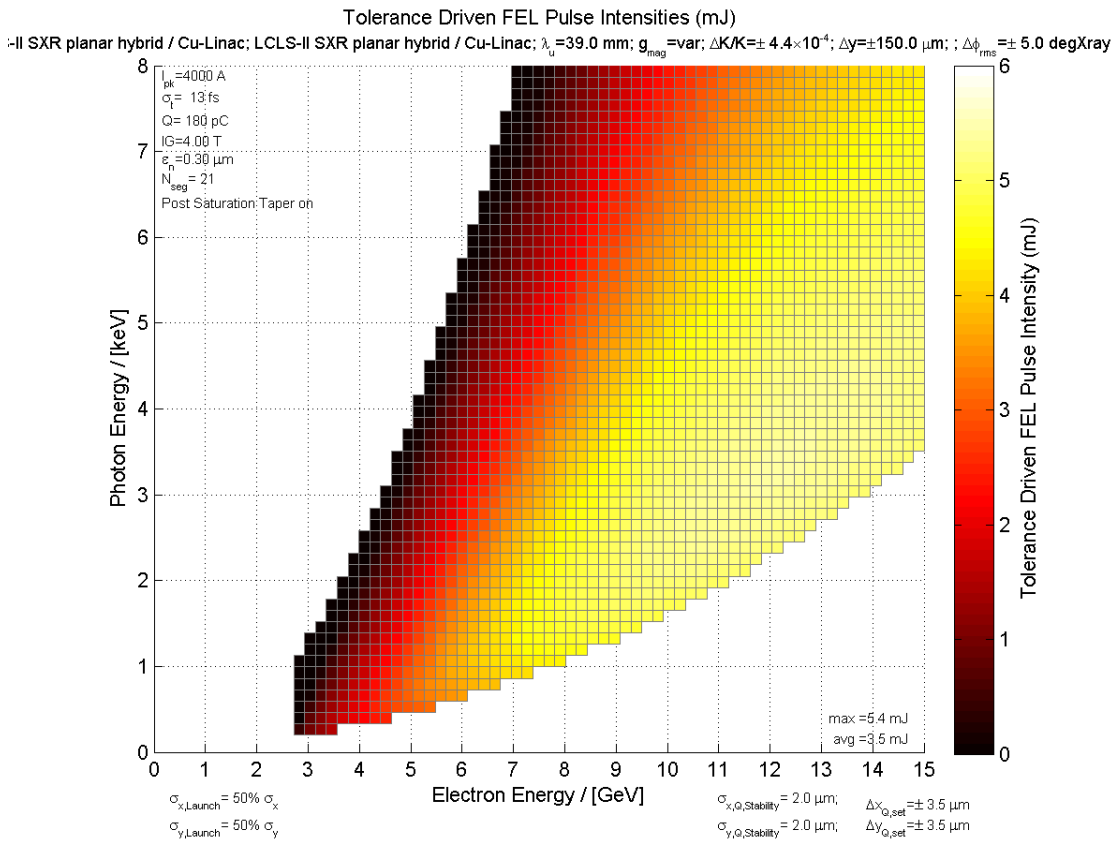

Figure 2: Semi-analytic prediction of the FEL performance. This plot shows the FEL pulse intensity as a function of both the electron beam energy (x-axis) and the photon energy (y-axis).

and the photon energy. For each electron beam energy, the gap adjustable undulator can be tuned to cover the indicated spectral range. The performance is impressive across the board. The total FEL pulse energy peaks at just over 5 mJ but shows an average pulse energy of 4-5 mJ for much of the tuning range.

2.4 Start-to-end simulations

The electron beam shown in Figure 1 is also used to evaluate the performance at the high end of the tuning range of the SXR undulator beamline, $E_\gamma = 1.5$ keV. This allowed for the

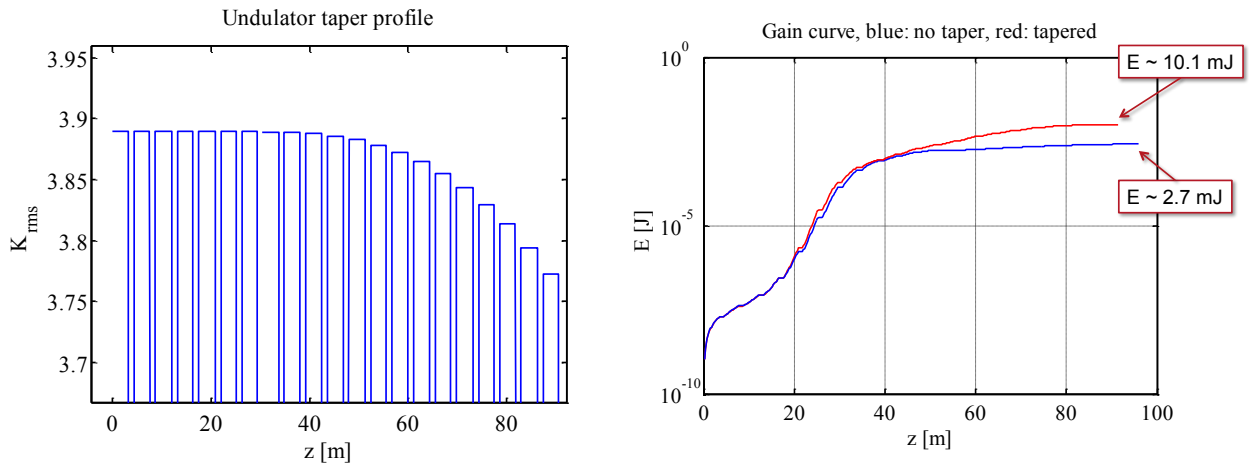

Figure 3: Optimized taper (left), gain curve (right).

highest energy electron beam ($\sim$ 10 GeV) as well as the largest undulator K value ($\sim$ 5.5). Time-dependent taper optimizations were done to evaluate the FEL performance with and without an optimal undulator taper. The optimal taper is shown in Figure 3 as well as the gain curves for both the tapered and untapered case. These simulations predict an impressive final energy of over 10 mJ.

The longitudinal characteristics of the FEL radiation in the case are equally impressive and are shown in Figure 4. The current horn in the tail of the electron beam produces

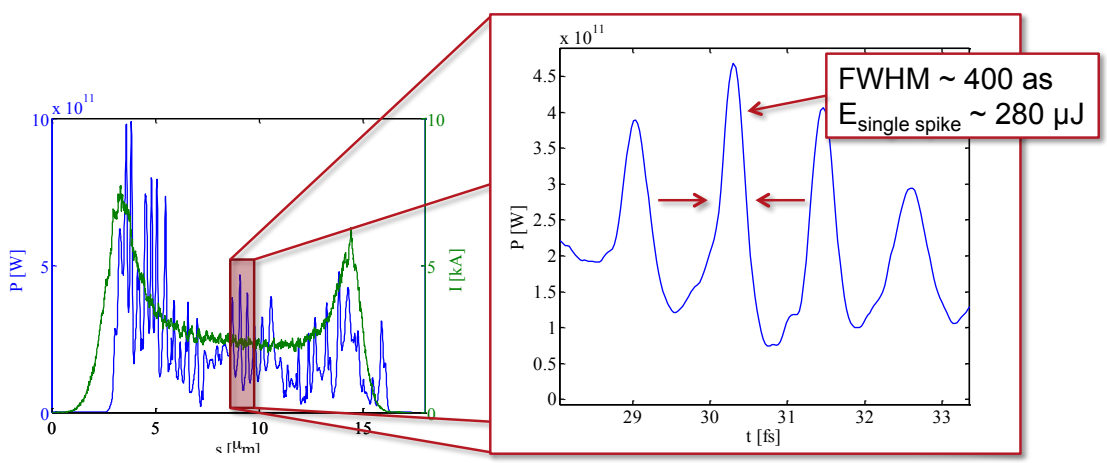

Figure 4: Left: Current (green) and power at the end of the undulator (blue). Right: zoomed view to show FEL pulse detail.

individual SASE spikes that approach peak powers of $\sim$ 1 TW. Individual SASE spikes have temporal durations of $\sim$ 400 attoseconds and contain roughly 280 μJ. Advanced schemes to slice of the electron beam could potentially be used to isolate individual spikes of radiation.

These schemes include, but are not limited to

- Electron beam emittance spoiling using a slotted foil
- Single-cycle laser modulation with undulator tapering
- Differential heating at the laser heater
- Various combinations of the above

Additionally, advanced schemes such as E-SASE and/or chirp and taper could potentially reduce the spike width further.

3 Cost estimate

The additional transport line taking the CuRF accelerated electron beam to the SXR undulator, including the associated beam transport optics, is estimated to cost on the order of $\sim$ \$5M. Additional cost, not estimated here, would be associated with any advanced schemes used to slice the electron beam and manipulate the FEL gain.

4 Conclusion

Feeding the LCLS-II SXR undulator with the low repetition rate but high power electron beam from the LCLS CuRF linac has been investigated. Semi-analytic results across a large tuning range have been reported. Furthermore, detailed quasi-start-to-end simulations of the high end of the SXR tuning range show extremely impressive FEL pulse characteristics. The beamline transport taking the electron beam from the CuRF linac to the LCLS-II SXR undulator has been designed. Additional start-to-end simulations will be needed to evaluate the impact, if any, of this transport on the FEL performance.

Acknowledgments

We thank A. Marinelli and Z. Huang for useful discussions.

References